Polyomic Analyses of Dopaminergic Neurons Isolated From Human Substantia Nigra in Parkinson's Disease: An Exploratory Study.

Affif ZACCARIA (zaccaria.affif@gmail.com)
University of Geneva Faculty of Medicine: Universite de Geneve Faculte de Medecine
https://orcid.org/0000-0001-9623-6269
Paola Antinori Malaspina
University of Geneva Medical Centre: Universite de Geneve Faculte de Medecine
Virginie Licker
University of Geneva Medical Centre: Universite de Geneve Faculte de Medecine
Enikö Kovari
University Hospital Geneva: Hopitaux Universitaires Geneve
Johannes A Lobrinus
University Hospital Geneva: Hopitaux Universitaires Geneve
Pierre R Burkhard
University Hospital Geneva: Hopitaux Universitaires Geneve

Research

Keywords: Parkinson's disease, human brain tissue, dopaminergic neurons, laser micro-dissection, Transcriptomics, Proteomics

Posted Date: February 12th, 2021

DOI: https://doi.org/10.21203/rs.3.rs-182873/v1

Polyomic analyses of dopaminergic neurons isolated from human substantia nigra in Parkinson's disease: An exploratory study.

Affif Zaccaria[1*], Paola Antinori[1], Virginie Licker[1], Enikö Kövari[2], Johannes A Lobrinus[3], Pierre R Burkhard[1,4].

[1] Neuroproteomics Group, University Medical Center, Faculty of Medicine, Geneva University, Geneva, Switzerland
[2] Department of Psychiatry, Geneva University Hospitals, Geneva, Switzerland
[3] Department of Pathology, Geneva University Hospitals, Geneva, Switzerland
[4] Department of Neurology, Geneva University Hospitals, Geneva, Switzerland

[*] Affif Zaccaria is the corresponding author
Affif Zaccaria and Paola Antinori are the co-first authors
Authors' declaration and Email addresses:
All authors of the manuscript have read and agreed to its content

affif.zaccaria@gmail.com
paola.antinori@gmail.com
virginie.licker@gmail.com
eniko.kovari@hcuge.ch
johannes.a.lobrinus@hcuge.ch
pierre.burkhard@hcuge.ch

Abstract

Background

Dopaminergic (DA) neurons of the substantia nigra pars compacta (SNpc) selectively and progressively degenerate in Parkinson's disease (PD). Until now, molecular analyses of DA neurons in PD have been limited to genomic and transcriptomic approaches, whereas, to the best of our knowledge, no proteomic or combined polyomic study examining the protein profile of these neurons, is currently available.

Methods

In this exploratory study, we used laser microdissection to extract DA neurons from 10 human SNpc samples obtained at autopsy in PD patients and control subjects. Extracted RNA and proteins were identified by RNA sequencing and nano-LC-MS/MS, respectively, and the differential expression between the PD and control group was assessed.

Results

Qualitative analyses confirmed that the microdissection protocol preserves the integrity of our samples and offers access to specific molecular pathways. This polyomic analysis highlighted differential expression of 52 genes and 33 proteins, including molecules of interest already known to be dysregulated in PD, such as *LRP2*, *PNMT*, *CXCR4*, *MAOA* and *CBLN1* genes, or the Aldehyde dehydrogenase 1 protein. On the other hand, despite the same samples were used for both analyses, correlation between RNA and protein expression was low, as exemplified by the CST3 gene encoding for the cystatin C protein.

Conclusion

This is the first exploratory study analyzing both gene and protein expression of LMD-dissected DA neurons from SNpc in PD. Although correlation between RNA and protein expressions was limited, this polyomic study provides an extensive and integrated overview of molecular changes identified in the PD SNpc and may offer novel insights into specific pathological processes at work in PD degeneration.

Key words : Parkinson's disease, human brain tissue, dopaminergic neurons, laser micro-dissection, Transcriptomics, Proteomics .

Background

Parkinson's disease[1] (PD) is the most common neurodegenerative movement disorder, currently affecting about seven million people worldwide. Despite decades of extensive basic and translational research, PD remains an incurable condition, and the cause and mechanisms of the degeneration of dopaminergic (DA) neurons in the substantia nigra pars compacta (SNpc) remains to be fully elucidated. Since the emergence of high throughput omics technologies some twenty years ago, several groups[2], including ours, have been able to study the molecular profile of post-mortem SN*pc* samples[3-6] with the purpose of identifying differential and specific molecular expression changes in PD compared to controls. Although these works allowed the in-depth molecular exploration of SN*pc* and the identification of altered signaling pathways such as inflammation[3], oxidative stress[4], proteasome, mitochondrial[5] or cell iron pathways[6], there is still no consensus about the molecular cascade at the basis of nigral DA degeneration in PD brains. Failure to dissect these approaches more specifically could be mainly related to the nature of samples under study i.e the whole SN*pc* specimens that were compared between control and PD groups. Indeed, the molecular analysis of whole PD SN*pc* mainly involved glial cells owing to the PD-related dramatically reduced component of DA neurons, whereas the molecular analysis of control SN*pc* integrated a higher proportion of DA neurons, resulting in unbalanced and biased comparisons.

Thus, a first step toward a better understanding of nigral degeneration would require specific molecular analyses of purified DA neurons from PD SNpc. In 2009, Simunovic et *al*[7] used laser microdissection (LMD) and RNA microarrays to analyze gene expression of dissected DA neurons from SN*pc* in PD samples. They identified a dysregulation of several known molecular regulatory pathways involved in PD pathogenesis such as oxidative stress-induced cell responses or dysfunction of the mitochondrial and ubiquitin-proteasome systems. However, this study, which focused on mRNA data only, revealed transcriptional activation of genes but did not inform about the protein expression level and function.

In 2016, the first proteomic study that focused on DA neurons was published by Plum et *al*[8]. By combining Laser Microdissection (LMD) with nano-lc-ms/ms, Plum et al.[8] identify 1'068 distinct proteins in DA neurons from healthy SNpc samples, but did not include PD samples in the study.

Therefore, to the best of our knowledge, there is still no published work applying quantitative proteomics to DA neurons from SNpc samples in PD, or simultaneously applying both transcriptomic and proteomic workflows to the same samples in PD.

Over the last decade, the progressive improvements of laser microdissection (LMD) technology[9] in automation, velocity and precision offers the opportunity to dissect frozen DA neurons in conditions that are more suitable for relevant molecular analyses. The increased sensitivity of mass spectrometers and RNA sequencers enables comparative and quantitative polyomic approaches using low to very low amounts of biological material.

In this exploratory study, we used LMD to dissect DA-neurons from control and PD post-mortem SNpc specimens. In the first part, we used both qualitative transcriptomic and proteomic approaches, to confirm the integrity and validity of our samples, and the LMD-provided access to the specific protein content of DA neurons. This important quality control step led to the second part of this study, where a quantitative comparison of protein and gene expression by label free approach and RNA sequencing (RNAseq), respectively, was performed in DA neurons from control and PD samples. Importantly, the same specimens were used for both analyses. RNAseq analysis revealed 52 differentially expressed genes, and label-free proteomics highlighted 33 differentially expressed proteins in PD samples compared to matched controls. Transcriptomics and proteomics results were compared to identify the mRNA-protein couples for which the expression changes followed the same direction. This work is the first attempt to propose a polyomic analysis of DA neurons in the PD brain.

Methods

Human brain tissues

Ten frozen human midbrains, 5 from age-matched control patients and 5 from PD patients were collected by the Department of Clinical Pathology and Psychiatry of the Geneva University Hospitals under a procedure approved by the Geneva ethical committee (Table 1) and in accordance with the relevant guidelines and regulations. Written informed consent for brain autopsy and use for research was obtained from close family relatives. PD diagnosis was confirmed neuropathologically and controls, with no previous history of neurological or psychiatric disorders, were confirmed to be free of nigral abnormalities. Samples were cryopreserved at -80°C until further analysis.

Table 1: **Summary for brain samples (PMI for Post Mortem Interval)**

Case ID	Primary diagnosis	Gender	Age (y)	PMI (h)	Proteomics	Transcriptomics
C1	Control	M	77	34	**x**	
C2	Control	M	85	31	**x**	
C3	Control	F	87	34	**x**	**x**
C4	Control	M	70	35	**x**	**x**
C5	Control	M	64	19	**x**	**x**
PD1	Parkinson's disease	M	79	17	**x**	
PD2	Parkinson's disease	M	84	38	**x**	**x**
PD3	Parkinson's disease	F	79	33	**x**	**x**
PD4	Parkinson's disease	M	73	25	**x**	
PD5	Parkinson's disease	M	73	25	**x**	**x**

Proteomic analysis

Laser Micro Dissection

12 µm tissue slices from each substantia nigra were cut at -18°C (Leica CM3050, Biosystems Switzerland AG, Muttenz, CH), mounted on 2 µm PEN membrane slides (Leica Biosystems Switzerland AG, Muttenz, Switzerland), fixed and dehydrated in ethanol. Collection of control and patient DA neurons was alternated to avoid a time-related bias.

DA neurons were visually identified by their brown neuromelanin pigment under bright field microscopy on a Leica LMD6000 instrument (Leica Microsystems GmbH, Wetzlar, Germany). Approximately 2,050 forms of DA neurons were accurately delimited at 200x magnification to reduce contamination by surrounding tissue, microdissected and catapulted into the vial cap in 8 µl of

RapiGest™ 0.1 % (Waters, GmbH, Milford, MA, USA) in TEAB 0.1 M (Sigma-Aldrich, Inc., St. Louis, MO), USA) The vial was vortexed upside-down, centrifuged to recover the sample at the bottom and sonicated with a VialTweeter UIS250v (Hielscher Ultrasonics GmbH, Teltow, Germany) to foster lysis and DA neuron detachment from the PEN membrane (70% amplitude, 0.5 sec cycle, 20 bursts, 5 times, on ice between each cycle). Samples were stored at -80°C.

Proteomic analysis with mass spectrometry

Microdissected DA neurons were thawed simultaneously, the volume was adjusted to 100 µl with lysis buffer (RapiGest™ 0.1 %Waters, Corporation, Milford, MA; TEAB 0.1 M; Sigma-Aldrich, Saint-Louis, MO) and protein concentration was estimated with a NanoDrop™ 2000 spectrophotometer (Waltham, Massachusetts, USA). For trypsin digestion the proteins were treated with TCEP 1 mM (Sigma-Aldrich, Saint-Louis, MO) (1 hour at 60°C; Sigma-Aldrich, Saint-Louis, US-MO) and iodoacetamide 4 mM (30 min at room temperature in the dark, shaking at 250 rpm, Sigma-Aldrich, Saint-Louis, MO), and trypsin (porcin, Promega Corporation, Madison, WI) was added to samples in a 1:25 ratio overnight. The reaction was stopped with 10% FA. RapiGest™ was removed by acid precipitation after incubation at 37°C for 40 min and centrifugation at 13,000 rpm for 20 min. The supernatant with the peptides was cleaned with a C18 microspin column (Harvard Apparatus, Holliston, MA) according to the manufacturer instructions, dried under speed-vacuum and stored at -80°C.

Mass spectrometry analysis was performed according to the protocol of the Proteomics Core Facility of the University of Geneva (https://www.unige.ch/medecine/proteomique/), as described by *Dor et al.*[10]

Peptide digests were solubilized in 5% acetonitrile and analyzed by electrospray ionization on a linear trap quadrupole (LTQ) Orbitrap velos Pro (Thermo Scientific, San Jose, CA, USA) equipped with a NanoAcquity system (Waters, Milford, MA, USA). Peptides were trapped on a home-made 5 µm 200 Å Magic C18 AQ (Michrom) 0.1 × 20 mm pre-column and separated on a commercial 0.075 x 150 mm

Nikkyo (Nikkyo Technology, Tokyo, JPN) analytical nanocolumn (C18, 5 µm, 100 Å). The analytical separation was run for 54 min (flow rate 200 nL/min) using a gradient as follows: 0-1 min 95 % A (0.1 %FA) and 5 % (99.9% acetonitrile, 0.1% formic acid) then to 65 % A and 35 % B for 55 min, and 20 % A and 80 % B at 65 min. For MS survey scans, the orbitrap (OT) resolution was set to 60,000 and the ion population was set to 5 × 105 with an m/z window from 400 to 2,000.

Three gas-phase fractions (GPF) for data-dependent MS/MS selection[11] were defined in the following m/z ranges: 400-598, 593-746 and 741-2,000 Th.

Five precursor ions were selected for collision-induced dissociation (CID) in the LTQ. The ion population was set to 1 × 104 (isolation width of 2 m/z) while for MS/MS detection in the OT, it was set to 1 × 105 with an isolation width of 2 m/z units. The normalized collision energies were set to 35% for CID.

Data analysis for proteomics

MaxQuant (version 1.5.8.3) was used to process Thermo raw files. For protein identification, data were searched against the UniProtKB/Swiss-Prot human database (release 2018_05, with 26,336 protein entries). N-terminal protein acetylation and methionine oxidation were set as variable modifications and cysteine carbamidomethylation as fixed. The default parameters were used for the instrument choice. Only one missed cleavage was allowed and search for second peptide matches and match between runs were activated. Peptides and protein FDR was set to 0.01. For protein quantification, label free quantification (LFQ) was chosen with a min. ratio count of 1 and unique + razor peptides were used. The other parameters were left as defaults.

Data analysis was performed using Perseus software. Common contaminants were filtered out and LFQ protein intensities were log2 transformed. At least 70% of protein intensities were required overall before imputing the missing values from a normal distribution. LFQ intensities were averaged across technical replicates before performing a two-sample t-test. Proteins with a p-value < 0.05 and a fold change > 1.5 were considered differentially expressed between patients and controls.

Gene expression analysis

LMD for gene expression analysis

For gene expression analysis we used 3 PD samples and 3 controls, for which SNpc was still available after proteomic sample preparation.

12 µm tissue slices from each substantia nigra were cut at -18°C and processed as described in the proteomic section. Approximately 70 forms of DA neurons were dissected in duplicates for each of the six different samples, and collected by gravity in distinct vials. The twelve resulting groups of DA neurons were quickly frozen on dry ice and stored at -80°C.

RNA extraction for quality control

Tissue depleted of DA neurons after LMD was also collected from the slides in 100 µL of lysis/denaturing buffer from the RNAqueous micro kit (Life technologies, Zug, Switzerland). RNAs were extracted following the manufacturer protocol, quantified with a Qbit™ fluorometer (Thermo Fisher, Waltham, MA, US) and analysed with an Agilent 2100 Bioanalyser (Agilent Technologies, Palo Alto, CA) to check the RNA profile and obtain the RNA Integrity number (RIN).

RNAseq library preparation and sequencing of NM-granules

The SMARTer™ Ultra Low RNA kit from Clontech was used for the reverse transcription and cDNA amplification according to the protocol described by *Vono et al.*[12], starting with 70 cells as input. Samples were defrozen simultaneously and solubilized in 10 µL of lysis buffer. After reverse transcription and amplification, 200 pg of cDNA were used for library preparation using the Nextera XT kit from Illumina. Library quality and molarity were assessed with the Qbit and Tapestation using a DNA High sensitivity chip (Agilent Technologies). Pools of 12 libraries were diluted at 2 nM for clustering on a Single-read Illumina Flow cell. Reads of 50 bases were generated using the TruSeq SBS chemistry on an Illumina HiSeq 4000 sequencer at the iGE3 Genomics Platform of the University of Geneva (https://ige3.genomics.unige.ch).

RNAseq data analysis

Sequencing quality control was performed with FastQC (v.0.11.5). Sequencing data were mapped to the UCSC human hg38 reference genome using STAR aligner (v.2.5.3a). The transcriptome metrics were evaluated with the Picard tools (v.1.141) and informed the decision to exclude 2 samples due to a low number of reads assigned to a gene.

The differential expression analysis PD /controls was carried out with the statistical Bioconductor package edgeR (v.3.14.0). The gene counts were normalized according to the library size. The genes having a count above 1 count per million reads (cpm) in at least 2 samples were carried forward for the analysis. The list of 26,485 genes was reduced to 22,561 after filtering out the poorly or not expressed genes. The differentially expressed gene tests were done with a GLM (general linear mode) with a negative binomial distribution. P-values were corrected for multiple testing error with a 5% FDR using the Benjamini-Hochberg procedure to retain only the significant genes.

In order to check whether the protein product of the differentially expressed genes has been already detected by MS, we generated a list of brain proteins with Nextprot[13] using the Advanced search (SPARQL) tool and querying for human proteins identified in the brain by MS with 2 distinct peptides 7 or more aminoacids long.

Results

Integrity and quality of samples by transcriptomics

Before proceeding to the quantitative comparisons between PD and control samples, we controlled that our sample preparation protocol preserved extracted molecules in sufficient quality for omics analyses. As RNAs are known to be more vulnerable entities than proteins, we used transcriptomic approaches to analyze RNA quality of our samples, by different ways, at different steps of the workflow.

To this purpose, tissue slices from SNpc of controls and PD patients (Table 1) were mounted on slides for laser microdissection of DA neurons (figure 1). About 70 DA neurons per sample were microdissected in duplicates and collected in distinct vials. For each sample, after dissection of DA

neurons, we collected on slide the remaining tissue into lysis buffer, extracted RNAs and determined their quality through observation of their electrophoretic profiles and the RIN measurement (figure 2). The electrophoretic profiles revealed an average RIN of 6.0 and 6.6 for PD and control samples, respectively. And although it showed decreased 18S and 28S peak intensity, peaks were clearly visible and positioned at the right nucleotide size (figure 2 and SI 1). In this context, we considered RNA quality as good enough to proceed to cDNA amplification with the SMARTer™ Ultra Low RNA kit. Starting with an average of 70 DA neurons per sample, the cDNA concentration obtained after amplification was homogeneous across all samples with an average cDNA concentration of 0.15 ± 0.01 ng/µl in PD samples and 0.16 ± 0.04 ng/µl in control samples and a global average cDNA concentration of 0.15 ± 0.03 ng /µl (SI-2). 200 pg of cDNA were used to generate one library for each individual sample. The average fragment size was 300bp and the fragments distribution was homogeneous across all samples, with no significant difference between control and PD groups (SI-2). Altogether, these results validated the sufficient quality and homogeneity of our samples, two important aspects before initiating quantitative comparisons between control and PD groups.

Assessment of LMD specificity by proteomics.

In order to validate the capacity of our protocol to specifically highlight the molecular content of DA neurons, we performed a proteomic analysis of the DA neurons collected from 5 control samples and 5 PD samples (Table 1). To obtain a sufficient amount of protein extract to perform triplicate injections for three gas-phase fractions[11](GPF) for data-dependent MS/MS selection, we dissected at 200x magnification an average of 2,050 DA neurons per sample (SI-1), covering an average area of 750,000 μm^2. To obtain this quantity of biological material, an average of 16 and 37 tissue sections were LMD-processed for control and PD samples, respectively.

The total amount of proteins extracted from these neurons ranged from 18 to 24 µg. 6 µg proteins of each sample were trypsin digested and injected in triplicates for three GPF runs with nano-lc-ms/ms. Data analysis with MaxQuant allowed the identification of 727 to 843 distinct proteins (Figure 3). The

comparison of these 10 protein-lists highlighted a total of 1,034 distinct proteins, identified by at least two proteotypic peptides (SI-3).

To confirm the quality of our DA-neuron enrichment using LMD approach, we compared our protein list with the list published by Plum *et al*[8]. These authors identified 1,068 distinct proteins, a figure very similar to our study. Interestingly, there was a 74% overlap between the two lists. In fact, 760 of the 1,034 proteins were identified in both studies. Then, to demonstrate that dissection of DA neurons, a subcompartment of SNpc, gave access to a specific subproteome, we compared our 1,034 proteins with the most exhaustive proteome of whole SN*pc*, published by our group in 2014[14], with a list of 1,795 different species (figure 4A and SI-4). On the one hand, among the 1,034 proteins identified into dissected DA neurons, 862 species were also identified into the whole SN*pc*. On the other hand, 170 proteins were only present into the DA neuron compartment. In fact, while these 170 proteins were identified in at least 80 % of DA neuron samples, they were never identified into the whole SN*pc* samples. Interestingly, the comparison of the whole SNpc with Plum et al.[8] revealed 864 common proteins, a number very similar to our study. And among the 170 DA neuron-specific proteins from our list, 80 were also identified by Plum et al.[8] These qualitative observations and comparisons with previous published studies suggest that our LMD-nano-lc-ms/ms protocol allowed access to a specific proteome of DA neurons, which, as anticipated, is not accessible with whole SNpc approaches.

In this first part of the study, we used transcriptomic and proteomic approaches (i) to confirm that our LMD-related sample preparation preserved samples in sufficient quality for molecular analyses and (ii) to validate that subcellular selection of DA neurons offered access to a specific subproteome. These results strengthened the interest for quantitative polyomics approaches to identify PD-related specific events in DA neurons.

Differential expression between control and PD samples.

To proceed to comparative analyses between PD and control samples through polyomic workflows, we first compared the mRNA abundance of 17,002 protein-coding genes between PD and control DA neurons (SI-5). A total of 52 genes (0.3%) showed significantly different gene expression at FDR p

values <0.05. In PD samples, RNA expression was increased for 40 genes and decreased for 12 genes (Table 2). Among these 52 differentially expressed genes, at least 10 genes are of particular interest: the upregulation of *MT1H, CXCR4, PNMT, BTG3, LRP2, AGT, S100B, MAOA* and *CST3* and the downregulation of *CBLN1* have been observed in previous studies investigating PD or other neurological disorders. Upregulated genes showed differences ranging from 3-fold change for *MAOA* to 98-fold change for *MT1H*, while *CBLN1* was downregulated with a 2.5-fold change.

Table 2: Differentially expressed genes between PD and control samples.

	Gene Name	Description	Fold Change PD/CTR	p-value	Identification of the corresponding protein in our study	Identification of the corresponding protein in any brain MS-studies
1	EHF	ETS homologous factor (hEHF)	193,4	3,2E-05	NO	**NO**
2	**MT1H***	Metallothionein-1H	98,3	3,3E-06	NO	**NO**
3	CHIT1	Chitotriosidase-1	79,1	1,4E-04	NO	YES
4	KCNJ8	ATP-sensitive inward rectifier potassium channel 8	40,9	6,5E-05	NO	**NO**
5	**CXCR4***	C-X-C chemokine receptor type 4	16,0	1,3E-04	NO	**NO**
6	**PNMT***	Phenylethanolamine N-methyltransferase	10,0	1,1E-04	NO	**NO**
7	**BTG3***	Protein BANP	8,3	2,5E-05	NO	**NO**
8	STC1	Stanniocalcin-1	7,6	7,4E-07	NO	**NO**
9	SLC18A1	Vesicular amine transporter 1	7,3	1,8E-05	NO	**NO**
10	**LRP2***	Low-density lipoprotein receptor-related protein 2	7,3	4,8E-05	NO	YES
11	NRP2	Neuropilin-2	7,2	1,2E-04	NO	YES
12	TGFBR3	Transforming growth factor beta receptor type 3	7,2	1,2E-04	NO	YES
13	EFEMP1	EGF-containing fibulin-like extracellular matrix protein 1	7,0	2,2E-06	NO	YES
14	ANTXR2	Anthrax toxin receptor 2	5,9	1,3E-04	NO	**NO**
15	JAM2	Junctional adhesion molecule B	5,6	4,1E-05	NO	YES
16	GJB6	Gap junction beta-6 protein	5,4	3,3E-05	NO	YES
17	COX7A1	Cytochrome c oxidase subunit 7A1, mitochondrial	5,2	8,8E-05	NO	YES
18	HHATL	Protein-cysteine N-palmitoyltransferase HHAT-like protein	5,2	9,3E-05	NO	YES
19	CNR1	Cannabinoid receptor 1	5,2	6,3E-05	NO	YES
20	CD99	CD99 antigen	4,8	8,3E-06	NO	YES
21	TMEM47	Transmembrane protein 47 (Brain cell membrane protein 1)	4,1	7,4E-07	NO	**NO**
22	CPM	Carboxypeptidase M	4,0	1,2E-04	NO	YES
23	**AGT***	Angiotensinogen (Serpin A8)	3,9	6,7E-05	NO	YES
24	NKAIN4	Sodium/potassium-transporting ATPase subunit beta-1-interacting protein 4	3,9	1,3E-04	NO	**NO**
25	ABCA1	ATP-binding cassette sub-family A member 1	3,9	1,3E-05	NO	**NO**
26	RGS5	Regulator of G-protein signaling 5	3,8	2,2E-05	NO	**NO**
27	**S100B***	Protein S100-B	3,7	1,1E-04	**YES**	YES
28	FGF14	Fibroblast growth factor 14	3,7	1,5E-04	NO	**NO**
29	LHFP	LHFPL tetraspan subfamily member 6 protein	3,6	4,8E-05	NO	**NO**
30	TTYH1	Protein tweety homolog 1 (hTTY1)	3,5	4,9E-05	NO	YES
31	**CST3***	Cystatin-C	3,4	2,7E-06	**YES**	YES
32	TEAD1	Transcriptional enhancer factor-1	3,3	4,4E-05	NO	**NO**
33	**MAOA***	Monoamine oxidase type A	3,2	1,6E-05	**YES**	YES
34	SLC1A2	Excitatory amino acid transporter 2	3,2	7,6E-07	**YES**	YES
35	PLEKHB1	Pleckstrin homology domain-containing family B member 1	3,1	5,3E-07	NO	YES
36	GATM	Glycine amidinotransferase, mitochondrial	2,8	6,7E-05	NO	YES
37	CHN2	Beta-chimaerin	2,8	2,3E-05	NO	YES
38	CADM1	Cell adhesion molecule 1	2,6	1,9E-05	NO	YES
39	PCSK2	Neuroendocrine convertase 2	1,9	2,1E-05	NO	YES

40	HSPH1	Heat shock protein 105 kDa	1,7	1,3E-04	**YES**	YES
41	SLC38A1	Sodium-coupled neutral amino acid transporter 1	0,7	1,1E-04	NO	**NO**
42	RABGAP1L	Rab GTPase-activating protein 1-like	0,7	7,9E-05	NO	YES
43	CCDC85A	Coiled-coil domain-containing protein 85A	0,6	1,5E-04	NO	YES
44	MACROD2	O-acetyl-ADP-ribose deacetylase MACROD2	0,6	1,0E-04	NO	YES
45	LPGAT1	Acyl-CoA:lysophosphatidylglycerol acyltransferase 1	0,6	1,1E-04	**YES**	YES
46	KANK4	KN motif and ankyrin repeat domain-containing protein 4	0,6	3,1E-05	NO	YES
47	FAM126A	Hyccin	0,5	3,3E-05	NO	YES
48	GSG1L	Germ cell-specific gene 1-like protein	0,5	1,4E-04	NO	YES
49	**CBLN1***	Cerebellin-1	0,4	6,1E-05	**YES**	YES
50	RGS16	Regulator of G-protein signaling 16	0,4	6,6E-05	NO	**NO**
51	RASGRF2	Ras-specific guanine nucleotide-releasing factor 2	0,3	2,5E-05	NO	YES
52	SSTR1	Somatostatin receptor type 1	0,3	4,8E-05	NO	**NO**

Genes marked with an asterisk (*) have been already reported as dysregulated in PD

Second, we compared protein expression between PD and control groups using label-free quantification. Among the 1,034 identified proteins, 33 (3.2%) were differentially expressed (T-test, p value<0.05) between PD and control, with at least a 1.5-fold change (Table 3), including 12 proteins with increased and 21 with decreased expression in PD samples. Among these 33 differentially expressed proteins, three upregulated, Cystatin-C, Cathepsin L1, Annexin A2, and two downregulated, Aldehyde dehydrogenase 1 and Alpha-1-antitrypsin, proteins in PD samples deserve a particular attention as they also appeared deregulated in previous publications involving PD or other neurological disorders. PD-overexpressed proteins showed differences ranging from 1.8-fold change for Cystatin-C to 3.5-fold change for Vimentin, while downregulated proteins showed differences ranging from 2.5-fold change for Aldehyde dehydrogenase 1 to 3.7-fold change for Alpha-1-antitrypsin.

Table 3: Differentially expressed proteins between PD and control samples.

	Gene Name	Protein Description	Fold Change PD/CTRL	p-value
1	VIM	Vimentin*	3,5	0,017
2	CTSL	Cathepsin L1*	3,0	0,033
3	GLIPR2	Golgi-associated plant pathogenesis-related protein 1	2,3	0,007
4	ANXA2	Annexin A2*	2,2	0,004
5	MBP	Myelin basic protein	1,8	0,028
6	CST3	Cystatin-C*	1,8	0,018
7	CPE	Carboxypeptidase E	1,8	0,037
8	PMP2	Myelin P2 protein	1,7	0,035
9	CNP	2,3-cyclic-nucleotide 3-phosphodiesterase	1,6	0,050
10	UBA52;RPS27A;UBB;UBC	Ubiquitin-60S ribosomal protein L40	1,6	0,020
11	ASRGL1	Isoaspartyl peptidase/L-asparaginase	1,5	0,029
12	GJA1	Gap junction alpha-1 protein	1,5	0,032
13	PRKAR2B	cAMP-dependent protein kinase type II-beta regulatory subunit	0,7	0,013
14	TIMM8A	Mitochondrial import inner membrane translocase subunit Tim8 A	0,7	0,040
15	VARS	Valine--tRNA ligase	0,6	0,038
16	STXBP5	Syntaxin-binding protein 5	0,6	0,044
17	MARS	Methionine--tRNA ligase, cytoplasmic	0,6	0,013
18	COPA	Coatomer subunit alpha	0,6	0,033
19	SNRPD3	Small nuclear ribonucleoprotein Sm D3	0,6	0,038

20	FKBP8	Peptidyl-prolyl cis-trans isomerase FKBP8	0,6	0,039
21	CKAP4	Cytoskeleton-associated protein 4	0,6	0,046
22	FXR2	Fragile X mental retardation syndrome-related protein 2	0,5	0,048
23	APOO	Apolipoprotein O	0,5	0,012
24	PDE10A	cAMP and cAMP-inhibited cGMP 3,5-cyclic phosphodiesterase 10A	0,5	0,043
25	NARS	Asparagine--tRNA ligase, cytoplasmic	0,5	0,041
26	NOMO2;NOMO1;NOMO3	Nodal modulator 2	0,5	0,009
27	GBE1	1,4-alpha-glucan-branching enzyme	0,5	0,012
28	DNAJB11	DnaJ homolog subfamily B member 11	0,5	0,020
29	FABP7	Fatty acid-binding protein, brain	0,4	0,028
30	CDS2	Phosphatidate cytidylyltransferase 2	0,4	0,034
31	ALDH1A1	Aldehyde dehydrogenase 1*	0,4	0,024
32	FKBP4	Peptidyl-prolyl cis-trans isomerase FKBP4	0,4	0,046
33	SERPINA1	Alpha-1-antitrypsin*	0,3	0,043

Proteins marked with an asterisk (*) have been already described in PD as dysregulated

Somewhat surprisingly, correlation of transcriptomic and proteomic analyses only revealed one common event: the *CST-3* gene and its corresponding translated protein Cystatin-C that were both significantly upregulated in PD samples. That was not the case for *S100 B* and *MAOA*, 2 upregulated genes in our study, as expression of their corresponding protein was not significantly different in PD samples. Concerning the 6 others interesting genes (*MT1H, CXCR4, PNMT, BTG3, LRP2, AGT*), their corresponding proteins were not identified by our proteomic workflow. To better understand the low correlation between transcriptomic and proteomic data, we focused on the proteins identified and quantified in our proteomic workflow and present in the list of the 52 differentially expressed genes. In fact, only 7 gene-related proteins (13.5%) were identified by nano-lc-ms/ms among the potential 52 gene products, whereas no corresponding protein for the 45 remaining deregulated genes could be found, making correlation between transcriptomic and proteomic data impossible. Among these 52 genes, 19 had never seen their corresponding protein identified by mass spectrometry from brain samples according to Nextprot database[13](Table 2).

In summary, this second part of the study was devoted to compare for the first time RNA and protein expressions from DA neurons, in PD and control SNc. These comparative analyses separately revealed relevant differences of expression in PD samples, supporting previous observations conducted in whole SNpc studies. However, correlation between transcriptomic and proteomic data was limited by our proteomic workflow. In fact, while the transcriptomic approach provided information about approximately 15,000 genes, the proteomic approach was limited to 1,000 proteins. Moreover, the

proteins corresponding to the majority of dysregulated genes were not identified by our nano-lc-ms/ms-related workflow.

Discussion

The difficulty to identify key molecular mechanisms at the basis of PD is a major obstacle to the development of neuroprotective therapies. DA neurons in the SNpc represent the main cellular compartment affected by degeneration in PD, and thus appear as relevant entities to isolate and analyze.

In this study, we used LMD to extract DA neurons from post-mortem control and PD SN*pc*. RNA-based analysis confirmed sufficient quality of all used samples for molecular analyses. A qualitative proteomic analysis of our samples showed high similarity with Plum *et al.*[8] who, using LMD-coupled nano-lc-MS/MS, provided an exhaustive proteome of DA neurons from healthy subjects. Our present study confirms the feasibility and the relevance of such workflow, and updates the human proteome of DA neurons with new identified proteins. Moreover, the comparison of our list with the whole SN*pc* proteome published by our group[14], confirmed that using LMD allows access to a specific subproteome, here composed of 170 species, which were not identified in the whole SNpc samples despite a protein fractionation protocol. These 170 proteins also update the human proteome of the SNpc.

We then applied both quantitative proteomic and transcriptomic workflows to our dissected DA neurons in order to identify specific molecular events in PD-related samples. To our knowledge, we are the first (1) to compare protein expression of DA neurons in PD and control samples, and (2) to apply both proteomic and transcriptomic workflows to microdissected DA neurons. The real challenge to perform this kind of comparative analysis relies on the high number of tissue sections required for PD samples. In fact, for each PD sample, an average of 37 tissue sections were microdissected in order to collect enough DA neurons. In total, more than 300 tissue sections were required for this polyomic

study. This information reflects the significant DA neuron loss observed in PD samples, and thus the highly challenging context to perform these experiments.

In our study the comparative analysis of gene expression revealed 52 dysregulated entities in PD samples, among which *LRP2* was upregulated. *LRP2* encodes for megalin receptor, also known as the neuronal receptor for metallothionein proteins, proteins whose function as metal exchanger would be neuroprotective for brain tissue. In PD context, gene expression of *LRP2*[15] has been previously reported to increase in nigral DA neurons.

PNMT, encoding for Phenylethanolamine N-methyltransferase was also upregulated in our study. Interestingly, Phenylethanolamine N-methyltransferase can induce, through its catalytic activity, cytotoxic N-methylated beta carbolineum cations, which have structural and functional similarity with neurotoxic 1-methyl-4-phenyl-pyridinium cation (MPP+). Several studies[16,17] have shown that within DA neurons, PNMT-induced beta carbolineum cations inhibit mitochondrial respiration. High PNMT catalytic activity has been observed in SNpc and locus coeruleus[18], the two most affected brain areas in PD. Thus, our results confirm previous observations and strengthen the hypothesis suggesting that increased levels of PNMT could induce neurotoxin-mediated death[19].

In PD brain, increased activation of microglia[20] releases pro-inflammatory molecules such as cytokines, and may contribute to neuronal damage observed in this disorder. Among cytokines, CXCR4 and its ligand CXCL12 are important members of the chemokine family, and are expressed in the central nervous system. In 2009, Shimoji et al.[20] demonstrated that CXCR4 was elevated in SNpc DA neurons, more in PD than in control samples. In the same study, the authors also suggested that increased CXCR4 expression occurs before and is not consecutive to DA neuronal loss. Thus, CXCR4 signaling would enhance the loss of DA neurons. In our study, we observed the upregulation of *CXCR4* gene expression in PD samples, confirming results from previous studies and the important role of inflammation in PD degeneration.

The enzyme monoamine oxidase A (MAOA) is a drug target in the treatment of PD[21]. The inhibition of MAO by drugs prevents dopamine breakdown, maintaining a higher level of dopamine into the brain

of PD patients. MAOA is principally located in neurons[22,23] , and is primarily responsible for dopamine metabolism in the latter. In 2017, Tong et al.[24] observed a 33% increase of the protein expression of MAOA in PD-related whole SN*pc*. Considering that MAOA is mainly expressed in dopamine neurons, which are reduced in PD conditions, Tong et al.[24] were surprised by these observations and proposed different explanations including the expression of MAOA by glial cells or an upregulation of MAOA into surviving DA neurons.

In our present study, we observed an increased expression of *MAOA* gene in PD DA neurons supporting an upregulation of MAOA into surviving DA neurons, although we cannot entirely exclude contamination by others cells. These results confirm previous observations and strengthen the interest toward MAO inhibitors for symptomatic purposes.

In our study, we observed a downregulation of *CBLN1*, that encodes for cerebellin 1 protein, in PD samples. In 2018, Zucca et al.[25] confirmed the expression of cerebellin-1 protein into DA neurons. *CBLN1* is among the most consistently reported downregulated genes across studies on PD[26-28]. Cerebellins are hexameric protein hormones with neuromodulator functions. Their physiological role is not entirely elucidated although it has been reported that cerebellins increase norepinephrine synthesis. Consequently, when not enough cerebellin is present in the brain, the level of dopamine might also decrease.

All these dysregulated genes have been previously described in others studies and are particularly interesting according to the function of the corresponding proteins. Unfortunately, the quantitative expression of these corresponding proteins could not be measured in our samples. In fact, while RNA seq provides a complete picture of all expressed transcripts and because low copy mRNAs are also amplified during the workflow, protein identification using non-targeted MS-related proteomics is limited by instrument-related dynamic range. Indeed, for 19 out of the 52 dysregulated genes, the protein product has never been identified by MS approaches. Moreover, among the 1,034 identified and quantified proteins, only 7 were encoded by genes we observed as dysregulated in our study. At

first glance, the low correlation between transcriptomic and proteomic data may seem odd but several previous studies have already confirmed this trend[29]. For example, in 2016, Dumitriu et al.[30] compared RNA and protein expression from post-mortem human prefrontal cortex in PD and control samples. Although 283 proteins and 1,095 mRNAs were significantly different between PD and controls, only 8 genes were in common and with the same direction effect between the two sets of results. Greenbaum et al.[29] propose at least three main reasons to explain poor correlation between mRNA and protein levels, including the multiple, complex and varied post-transcriptional mechanisms involved in turning mRNA into protein, the difference in *in vivo* half-lives between RNA and protein, and the significant amount of error and noise in both protein and mRNA experiments.

Nevertheless, despite this poor correlation, our proteomic analysis also revealed dysregulated proteins of interest in PD samples. Indeed, in our study, the expression of cystatin C protein was increased in PD samples, and followed the same direction of expression as its gene, CST3. Cystatin C is an endogenous inhibitor of cysteine proteases such as cathepsins B, H, K, S and L, and is present in all mammalian body fluid and tissues[31]. Increased expression of cystatin C in cerebrospinal fluid has been highlighted in many neurodegenerative disorders[32], including Alzheimer's disease[33], and it was suggested to be of diagnostic interest. In PD, Xu et al.[34] demonstrated an overexpression of the CST3 gene and higher levels of cystatin C in DA-depleted rat striatum. In the same line, we here describe for the first time an increased cystatin gene and protein expressions in human DA neurons of PD patients. Recent *in vitro*[35-37] and *in vivo*[34,38] results have suggested a neuroprotective role of cystatin C. In fact, administration of human cystatin C into the rat SN*pc* partially rescued DA neurons following a 6-OHDA-induced lesion[34]. This neuroprotective function of cystatin C may be related to its inhibitory action on cathepsins and/or to induction of autophagy.

In our study we also observed a decreased expression of aldehyde dehydrogenase 1 in PD samples. Encoded by ALDH1A gene, Aldehyde dehydrogenase 1 is a detoxification enzyme that participates in the metabolism of both dopamine (DA) and norepinephrine. It is exclusively expressed in DA neurons where it converts by oxidation a toxic metabolite of dopamine, the 3,4 dihydroxyphenylacetaldehyde

(DOPAL) into a non-toxic form, the dihydrophenylacetic acid (DOPAC). In 2003, Galter et al.[39] observed a decreased expression of ALDH1Aa mRNA in DA neurons of SNpc from PD patients, while DA neurons of VTA from the same patients were unaffected. Here our study reveals for the first time a decreased expression of its gene product Aldehyde dehydrogenase 1. We could interpret this finding in two different ways. First, decreased expression of Aldehyde dehydrogenase 1 in SNpc DA neurons of PD patients might be a consequence of PD-related degenerative process and thus a compensatory mechanism to slow down the rate of DA neuron degradation. Alternatively, this decreased expression of Aldehyde dehydrogenase 1 could also contribute to PD-related degeneration by allowing accumulation of DOPAL and aldehyde toxicity in DA neurons. Further studies are still necessary to appreciate whether decreased expression of Aldehyde dehydrogenase 1 may be involved in the development or the perpetuation of PD pathomechanisms.

Conclusion

This exploratory study is the first to generate proteomic and transcriptomic data from DA neurons in PD SNpc and results reported above underline the potential interest of such combined molecular approaches However, this study has also limitations, including a small set of samples and all expression changes reported above should be confirmed in more PD samples. Furthermore, although remaining the gold standard to decipher brain molecular alterations, autopsied tissues are associated with several drawbackss including difficulty to collect them and risks of degradation and contamination by agonal or post- mortem changes[40,41]. In fact, a massive and spreading depolarization of neurons with a high release of glutamate and potassium[42,43] has been described shortly before brain death. This phenomenon probably changes molecular expression in neurons, independently of PD-related events. Moreover, the post mortem interval has also an impact on RNA[41] and protein[40] expression. Therefore, it may seem that the ultimate sample for research in human PD has to be safely obtained from a large number of living individuals, and sampling-to-freezer time should be kept as short as possible. Brain tissue imprints[44] that can be collected during deep brain stimulation surgery appear promising samples for future studies using RNA sequencing or proteomics.

Supplementary information

Supplementary information accompanies this paper at

Abbreviations

SN*pc*: substantia nigra *pars compacta;* **PD:** Parkinson's disease; **DA:** dopaminergic neurons; **LMD**: laser microdissection; **LFQ**: label-free quantification; **RIN**: RNA integrity number; **GFP**: gaz-phase fractions; **LC:** liquid chromatography; **MS:** mass spectrometry

Acknowledgements

We thank the Histology, Bioimaging, Genomic and Proteomic Core Facilities for their technical support and willingness to help.

Our gratitude goes also to Michele El Atifi for her suggestions on the matter of the RNA analysis.

Author's contributions

AZ, VL and PRB designed the study. VL and PA performed the experiment. JAL and EK collected human specimens and confirmed the neuropathological diagnostic. AZ and PA analyzed the data. AZ, PA and PRB drafted the manuscript. All the authors have seen and approved the final version of the manuscript.

Funding

This work was supported by the Swiss National Science Foundation 31003A_143987 and Parkinson Swiss

Availability of data and materials

All data relevant to the study are included in the article or as supplementary information. Upon reasonable request, additional information will be shared by the corresponding authors.

Ethics approval

Midbrain tissues were obtained from the Division of Clinical Pathology and Psychiatry of the Geneva University Hospitals under a procedure approved by the local ethical committee. Written consents for brain autopsy and use for research purpose were signed by close relatives.

Consent for publication

All authors of the manuscript have read and agreed to its content

Competing interests

The authors declare that they have no competing interests

References

1 Kalia, L. V. & Lang, A. E. Parkinson's disease. *Lancet* **386**, 896-912, doi:10.1016/S0140-6736(14)61393-3 (2015).

2 Redensek, S., Dolzan, V. & Kunej, T. From Genomics to Omics Landscapes of Parkinson's Disease: Revealing the Molecular Mechanisms. *OMICS* **22**, 1-16, doi:10.1089/omi.2017.0181 (2018).

3 McGeer, P. L. & McGeer, E. G. Inflammation and neurodegeneration in Parkinson's disease. *Parkinsonism Relat Disord* **10 Suppl 1**, S3-7, doi:10.1016/j.parkreldis.2004.01.005 (2004).

4 Jenner, P. Oxidative stress in Parkinson's disease. *Ann Neurol* **53 Suppl 3**, S26-36; discussion S36-28, doi:10.1002/ana.10483 (2003).

5 McNaught, K. S., Olanow, C. W., Halliwell, B., Isacson, O. & Jenner, P. Failure of the ubiquitin-proteasome system in Parkinson's disease. *Nat Rev Neurosci* **2**, 589-594, doi:10.1038/35086067 (2001).

6 Berg, D. *et al.* Brain iron pathways and their relevance to Parkinson's disease. *J Neurochem* **79**, 225-236, doi:10.1046/j.1471-4159.2001.00608.x (2001).

7 Simunovic, F. *et al.* Gene expression profiling of substantia nigra dopamine neurons: further insights into Parkinson's disease pathology. *Brain* **132**, 1795-1809, doi:10.1093/brain/awn323 (2009).

8 Plum, S. *et al.* Proteomic characterization of neuromelanin granules isolated from human substantia nigra by laser-microdissection. *Sci Rep* **6**, 37139, doi:10.1038/srep37139 (2016).

9 Espina, V., Heiby, M., Pierobon, M. & Liotta, L. A. Laser capture microdissection technology. *Expert Rev Mol Diagn* **7**, 647-657, doi:10.1586/14737159.7.5.647 (2007).

10 Dor, M. *et al.* Investigation of the global protein content from healthy human tears. *Exp Eye Res* **179**, 64-74, doi:10.1016/j.exer.2018.10.006 (2019).

11 Scherl, A. *et al.* Genome-specific gas-phase fractionation strategy for improved shotgun proteomic profiling of proteotypic peptides. *Anal Chem* **80**, 1182-1191, doi:10.1021/ac701680f (2008).

12 Vono, M. *et al.* Maternal Antibodies Inhibit Neonatal and Infant Responses to Vaccination by Shaping the Early-Life B Cell Repertoire within Germinal Centers. *Cell Rep* **28**, 1773-1784 e1775, doi:10.1016/j.celrep.2019.07.047 (2019).

13 Gaudet, P. *et al.* The neXtProt knowledgebase on human proteins: 2017 update. *Nucleic Acids Res* **45**, D177-D182, doi:10.1093/nar/gkw1062 (2017).

14 Licker, V. *et al.* Proteomic analysis of human substantia nigra identifies novel candidates involved in Parkinson's disease pathogenesis. *Proteomics* **14**, 784-794, doi:10.1002/pmic.201300342 (2014).

15 Michael, G. J. *et al.* Up-regulation of metallothionein gene expression in parkinsonian astrocytes. *Neurogenetics* **12**, 295-305, doi:10.1007/s10048-011-0294-5 (2011).

16 Drucker, G., Raikoff, K., Neafsey, E. J. & Collins, M. A. Dopamine uptake inhibitory capacities of beta-carboline and 3,4-dihydro-beta-carboline analogs of N-methyl-4-phenyl-1,2,3,6-tetrahydropyridine (MPTP) oxidation products. *Brain Res* **509**, 125-133 (1990).

17 Matsubara, K. *et al.* Endogenously occurring beta-carboline induces parkinsonism in nonprimate animals: a possible causative protoxin in idiopathic Parkinson's disease. *J Neurochem* **70**, 727-735 (1998).

18 Kopp, N. *et al.* Distribution of adrenaline-synthesizing enzyme activity in the human brain. *J Neurol Sci* **41**, 397-409 (1979).
19 Gearhart, D. A., Neafsey, E. J. & Collins, M. A. Phenylethanolamine N-methyltransferase has beta-carboline 2N-methyltransferase activity: hypothetical relevance to Parkinson's disease. *Neurochem Int* **40**, 611-620 (2002).
20 Shimoji, M., Pagan, F., Healton, E. B. & Mocchetti, I. CXCR4 and CXCL12 expression is increased in the nigro-striatal system of Parkinson's disease. *Neurotox Res* **16**, 318-328, doi:10.1007/s12640-009-9076-3 (2009).
21 Miklya, I. The significance of selegiline/(-)-deprenyl after 50 years in research and therapy (1965-2015). *Mol Psychiatry* **21**, 1499-1503, doi:10.1038/mp.2016.127 (2016).
22 Finberg, J. P. & Rabey, J. M. Inhibitors of MAO-A and MAO-B in Psychiatry and Neurology. *Front Pharmacol* **7**, 340, doi:10.3389/fphar.2016.00340 (2016).
23 Levitt, P., Pintar, J. E. & Breakefield, X. O. Immunocytochemical demonstration of monoamine oxidase B in brain astrocytes and serotonergic neurons. *Proc Natl Acad Sci U S A* **79**, 6385-6389, doi:10.1073/pnas.79.20.6385 (1982).
24 Tong, J. *et al.* Brain monoamine oxidase B and A in human parkinsonian dopamine deficiency disorders. *Brain* **140**, 2460-2474, doi:10.1093/brain/awx172 (2017).
25 Zucca, F. A. *et al.* Neuromelanin organelles are specialized autolysosomes that accumulate undegraded proteins and lipids in aging human brain and are likely involved in Parkinson's disease. *NPJ Parkinsons Dis* **4**, 17, doi:10.1038/s41531-018-0050-8 (2018).
26 Grunblatt, E. *et al.* Gene expression profiling of parkinsonian substantia nigra pars compacta; alterations in ubiquitin-proteasome, heat shock protein, iron and oxidative stress regulated proteins, cell adhesion/cellular matrix and vesicle trafficking genes. *J Neural Transm (Vienna)* **111**, 1543-1573, doi:10.1007/s00702-004-0212-1 (2004).
27 Mandel, S. A., Fishman, T. & Youdim, M. B. Gene and protein signatures in sporadic Parkinson's disease and a novel genetic model of PD. *Parkinsonism Relat Disord* **13 Suppl 3**, S242-247, doi:10.1016/S1353-8020(08)70009-9 (2007).
28 Moran, L. B. *et al.* Whole genome expression profiling of the medial and lateral substantia nigra in Parkinson's disease. *Neurogenetics* **7**, 1-11, doi:10.1007/s10048-005-0020-2 (2006).
29 Greenbaum, D., Colangelo, C., Williams, K. & Gerstein, M. Comparing protein abundance and mRNA expression levels on a genomic scale. *Genome Biol* **4**, 117, doi:10.1186/gb-2003-4-9-117 (2003).
30 Dumitriu, A. *et al.* Integrative analyses of proteomics and RNA transcriptomics implicate mitochondrial processes, protein folding pathways and GWAS loci in Parkinson disease. *BMC Med Genomics* **9**, 5, doi:10.1186/s12920-016-0164-y (2016).
31 Bobek, L. A. & Levine, M. J. Cystatins--inhibitors of cysteine proteinases. *Crit Rev Oral Biol Med* **3**, 307-332 (1992).
32 Yamamoto-Watanabe, Y. *et al.* Quantification of cystatin C in cerebrospinal fluid from various neurological disorders and correlation with G73A polymorphism in CST3. *Brain Res* **1361**, 140-145, doi:10.1016/j.brainres.2010.09.033 (2010).
33 Deng, A., Irizarry, M. C., Nitsch, R. M., Growdon, J. H. & Rebeck, G. W. Elevation of cystatin C in susceptible neurons in Alzheimer's disease. *Am J Pathol* **159**, 1061-1068, doi:10.1016/S0002-9440(10)61781-6 (2001).

34 Xu, L. *et al.* Cystatin C prevents degeneration of rat nigral dopaminergic neurons: in vitro and in vivo studies. *Neurobiol Dis* **18**, 152-165, doi:10.1016/j.nbd.2004.08.012 (2005).
35 Hasegawa, A. *et al.* Regulation of glial development by cystatin C. *J Neurochem* **100**, 12-22, doi:10.1111/j.1471-4159.2006.04169.x (2007).
36 Kumada, T., Hasegawa, A., Iwasaki, Y., Baba, H. & Ikenaka, K. Isolation of cystatin C via functional cloning of astrocyte differentiation factors. *Dev Neurosci* **26**, 68-76, doi:10.1159/000080714 (2004).
37 Tizon, B. *et al.* Induction of autophagy by cystatin C: a mechanism that protects murine primary cortical neurons and neuronal cell lines. *PLoS One* **5**, e9819, doi:10.1371/journal.pone.0009819 (2010).
38 Kaur, G. *et al.* Cystatin C prevents neuronal loss and behavioral deficits via the endosomal pathway in a mouse model of down syndrome. *Neurobiol Dis* **120**, 165-173, doi:10.1016/j.nbd.2018.08.025 (2018).
39 Galter, D., Buervenich, S., Carmine, A., Anvret, M. & Olson, L. ALDH1 mRNA: presence in human dopamine neurons and decreases in substantia nigra in Parkinson's disease and in the ventral tegmental area in schizophrenia. *Neurobiol Dis* **14**, 637-647 (2003).
40 Crecelius, A. *et al.* Assessing quantitative post-mortem changes in the gray matter of the human frontal cortex proteome by 2-D DIGE. *Proteomics* **8**, 1276-1291, doi:10.1002/pmic.200700728 (2008).
41 Li, J. Z. *et al.* Systematic changes in gene expression in postmortem human brains associated with tissue pH and terminal medical conditions. *Hum Mol Genet* **13**, 609-616, doi:10.1093/hmg/ddh065 (2004).
42 Carlson, A. P. *et al.* Terminal spreading depolarizations causing electrocortical silencing prior to clinical brain death: case report. *J Neurosurg*, 1-7, doi:10.3171/2018.7.JNS181478 (2018).
43 Dreier, J. P. *et al.* Terminal spreading depolarization and electrical silence in death of human cerebral cortex. *Ann Neurol* **83**, 295-310, doi:10.1002/ana.25147 (2018).
44 Zaccaria, A. *et al.* Deep brain stimulation-associated brain tissue imprints: a new in vivo approach to biological research in human Parkinson's disease. *Mol Neurodegener* **11**, 12, doi:10.1186/s13024-016-0077-4 (2016).

Figure legends

Figure 1. LMD capture of DA neurons from a section of substantia nigra tissue mounted on a PEN membrane slide. (A) DA neurons (pointed by the green arrows) can be visually identified by their brown pigment (50x magnification). The black rectangle highlights the region depicted in figures (B-D) at 200x magnification. (C) The green lines define the DA neurons to guide the laser beam. (D) The shapes appear empty after cutting and collecting the granules in the tube cap situated under the slide.

Figure 2. Quality control of RNA extracted from DA neurons in PD and control samples. The electrophoretic profiles and the resulting RNA Integrity Number (RIN) were obtained to confirm integrity of all samples and were compared between control and PD samples.

Figure 3: Number of proteins identified in DA neurons of post-mortem SNpc by nano-lc-ms/ms: across all analysed samples (Total), in control samples (C1 to C5) and Parkinson's disease samples (PD1 to PD5).

Figure 4. Qualitative comparison of proteins identified from DA neurons with whole SNpc. Venn diagram representing both common and specific proteins identified in whole SNpc and DA neurons.

Figures

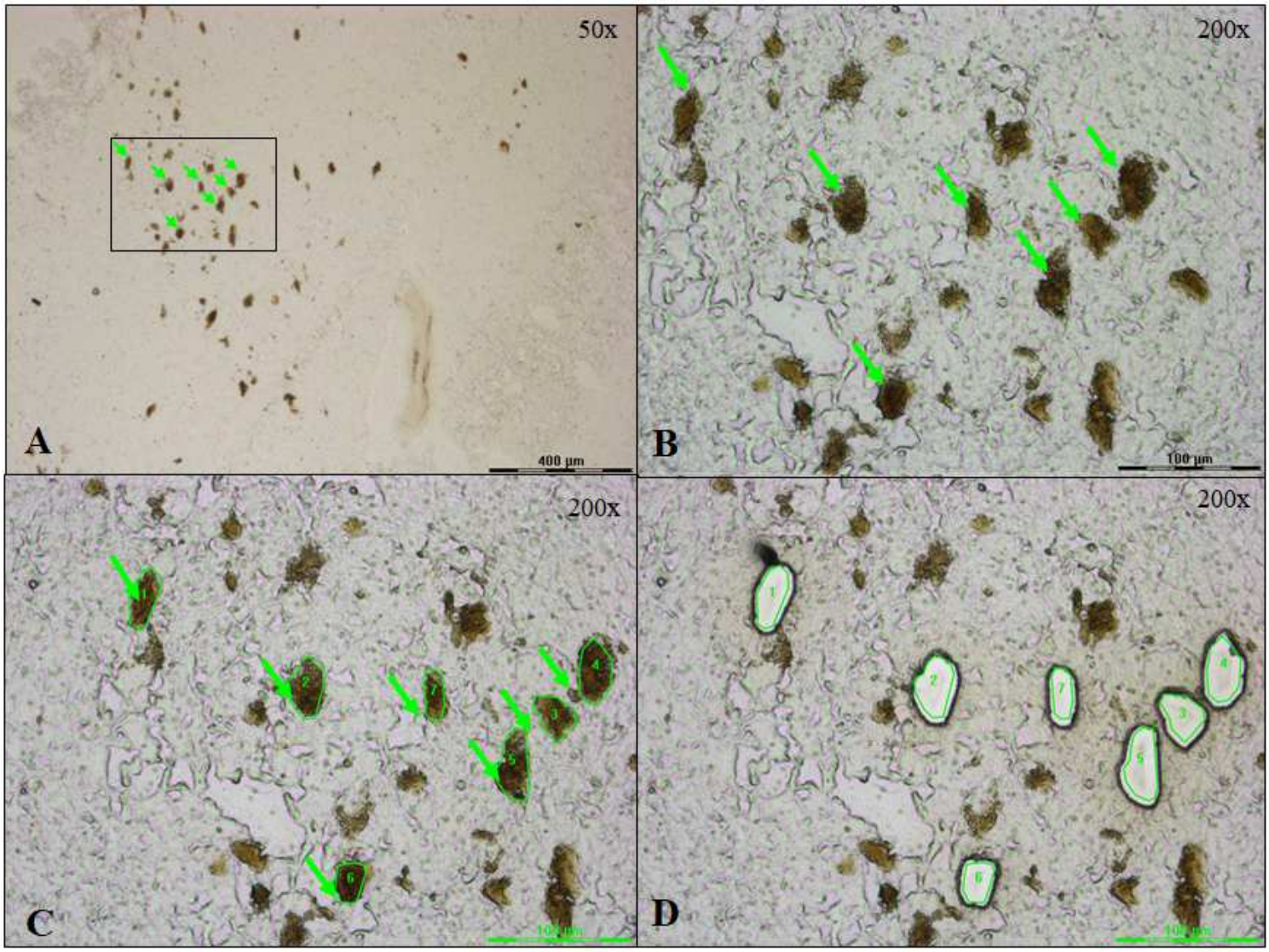

Figure 1

LMD capture of DA neurons from a section of substantia nigra tissue mounted on a PEN membrane slide. (A) DA neurons (pointed by the green arrows) can be visually identified by their brown pigment (50x magnification). The black rectangle highlights the region depicted in figures (B-D) at 200x magnification. (C) The green lines define the DA neurons to guide the laser beam. (D) The shapes appear empty after cutting and collecting the granules in the tube cap situated under the slide.

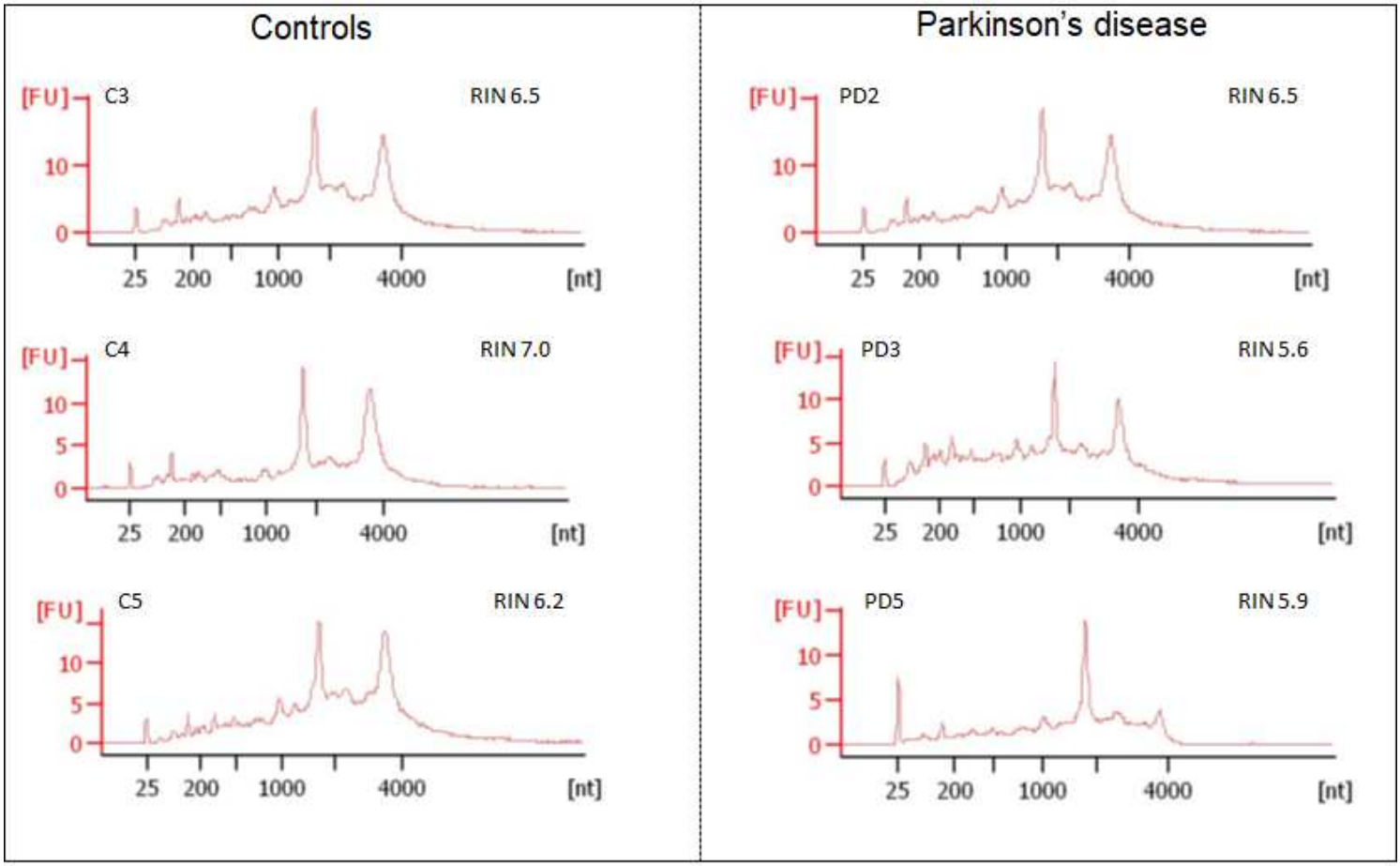

Figure 2

Quality control of RNA extracted from DA neurons in PD and control samples. The electrophoretic profiles and the resulting RNA Integrity Number (RIN) were obtained to confirm integrity of all samples and were compared between control and PD samples.

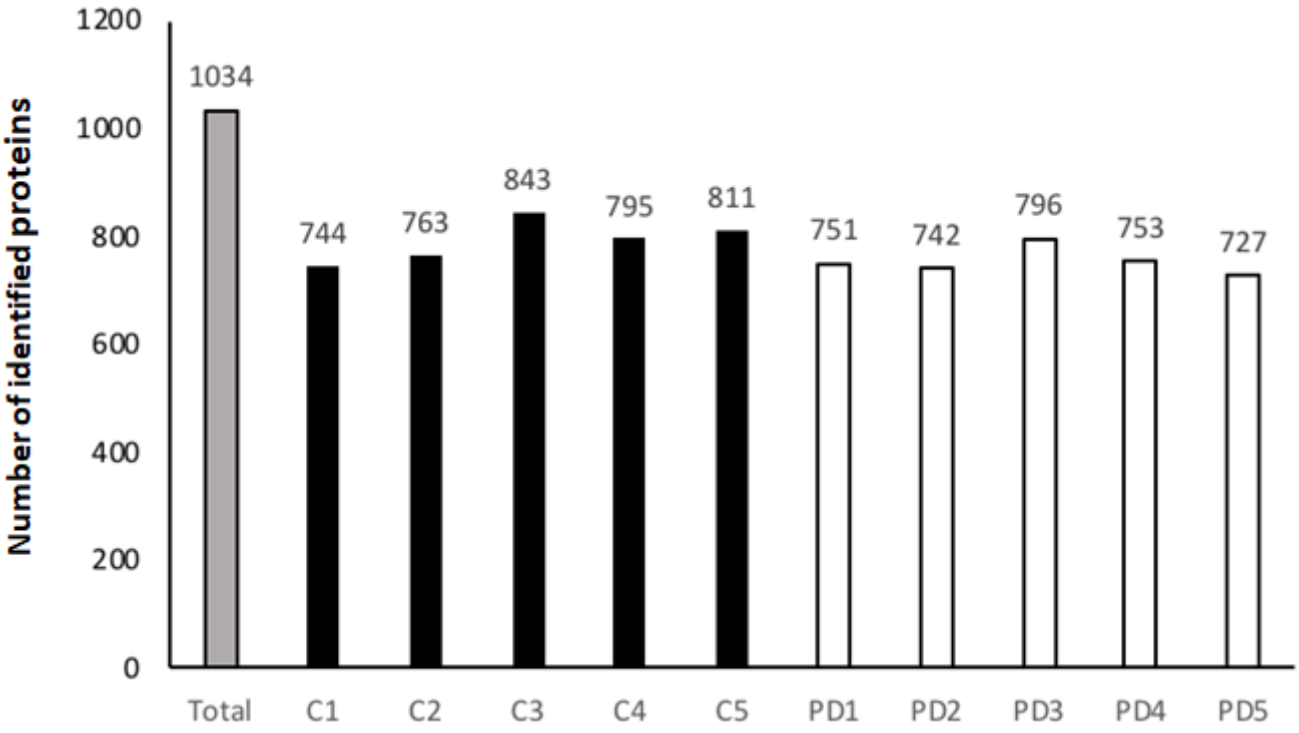

Figure 3

Number of proteins identified in DA neurons of post-mortem SNpc by nano-lc-ms/ms: across all analysed samples (Total), in control samples (C1 to C5) and Parkinson's disease samples (PD1 to PD5).

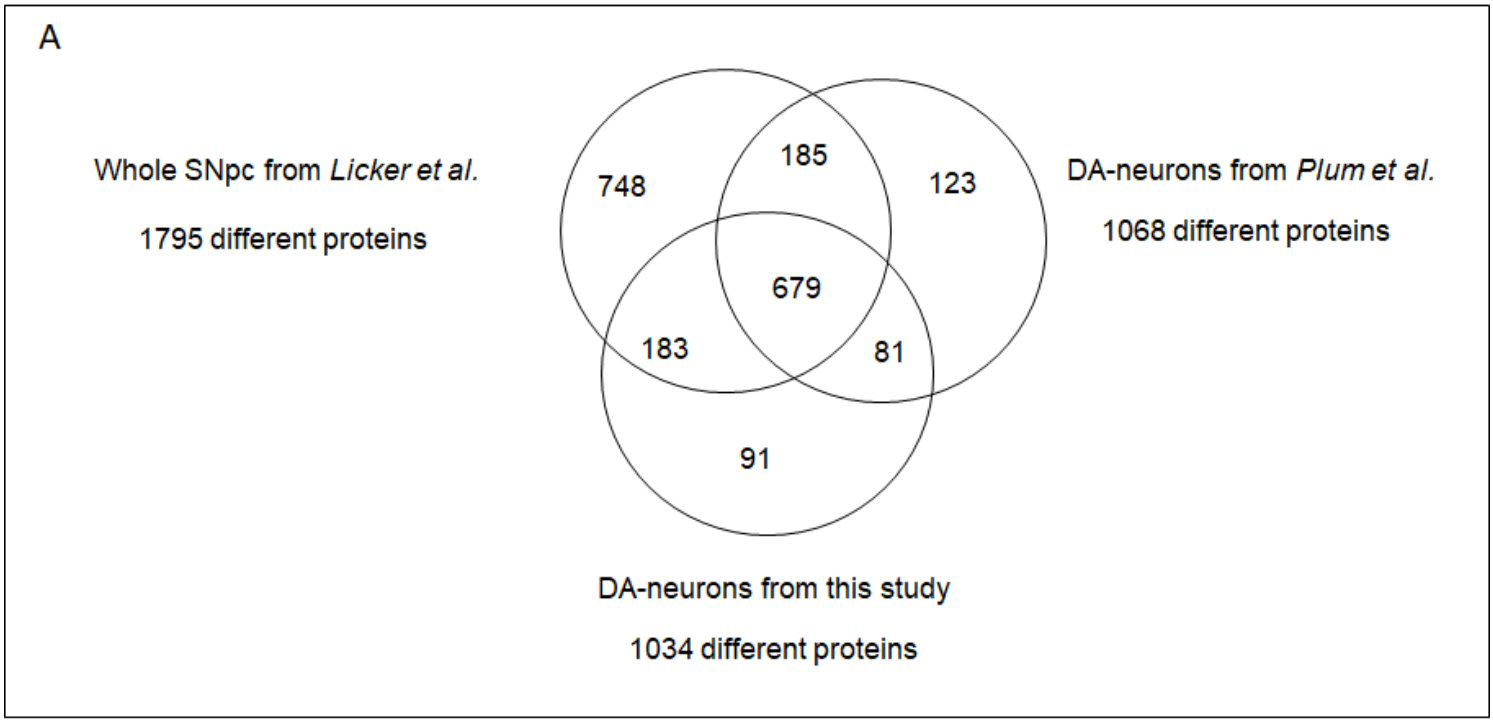

Figure 4

Qualitative comparison of proteins identified from DA neurons with whole SNpc. Venn diagram representing both common and specific proteins identified in whole SNpc and DA neurons.